PRAMANA — journal of physics
© Indian Academy of Sciences
Vol. 75, No. 5
November 2010
pp. 953–959

Development of a 16 kHz repetition rate, 110 W average power copper HyBrID laser

R BISWAL*, P K AGRAWAL, G K MISHRA, S V NAKHE, S K DIXIT and J K MITTAL
Laser Systems Engineering Division, Raja Ramanna Centre for Advanced Technology, Indore 452 013, India
*Corresponding author. E-mail: rbiswal@rrcat.gov.in

Abstract. This paper presents the design and performance analysis of an indigenously developed 110 W average output power copper HyBrID laser operating at 16 kHz pulse repetition rate. The laser active medium was confined within a fused silica tube of ∼6 cm diameter and ∼200 cm active length. An in-house developed high-power (∼10 kW) solid-state pulser was used as the electrical excitation source. A simple estimation of deposited electrical power, at the laser head, was carried out and based on it, the laser tube efficiency was found to be 2.9% at 70 W and 2.2% at 110 W laser power levels.

Keywords. Copper HyBrID laser; high repetition-rate laser; pulsed discharge; hydrogen bromide.

PACS Nos 42.55.Lt; 42.55.-f; 42.60.Jf; 52.80.-s

1. Introduction

Visible lasers with high average power (∼100 W), high pulse repetition rate (15–20 kHz) and short pulse duration (∼50 ns) are very appropriate pump sources of tunable dye lasers because of their further applications in laser isotope separation [1]. The choice of the pump laser is limited to either frequency-doubled Nd:YAG laser or a copper vapour laser (CVL). The CVL system offers visible beams with high beam quality and high average power without going to the route of frequency up-conversion. Copper HyBrID laser [2,3], an advanced variant of CVL, is a low-temperature (∼550°C), high pulse repetition rate (15–20 kHz), short start-up time (10–15 min) and high efficiency (1–3%) device with improved beam characteristics [1]. Because of the lower working temperature, a copper HyBrID laser is compact, light weight and air cooled even at high average power in contrast to higher-temperature (1500–1600°C), water-cooled CVL versions. Till now, the highest reported power from a copper HyBrID laser oscillator is 216 W with 19.5 l active volume and employing a 50 kW rated solid-state power supply [3]. In active volume ranging from 2.5 to 6 l, the laser power in the range of 80–200 W was reported

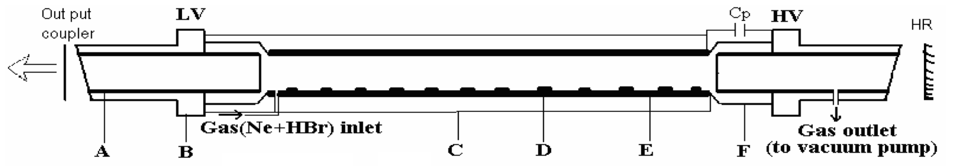

Figure 1. Schematic lay-out of the copper HyBrID laser. LV – low voltage side, HV – high voltage side, A – press-fitted Cu electrode, B – water-cooled SS flange, C – aluminium strips for current return, D – high purity Cu pieces, E – alumina fibre insulation, F – flared end fused silica discharge tube, Cp – peaking capacitor and HR – high reflector ($R > 99.9\%$).

[2–5]. The laser power from different models differ because of different active volumes, power supply ratings, electrical excitation schemes, ways of controlling the cavity losses and gas composition. In the past, we developed several models of copper HyBrID lasers delivering average powers of 30–60 W over a wide range of pulse repetition rates (15–27 kHz) [6,7].

This paper presents the design and performance characteristics of an indigenously developed copper HyBrID laser delivering an average power of 110 W with 2.2% tube efficiency at 16 kHz pulse repetition rate. The active volume was 5.5 l and an in-house-developed 10 kW rated solid-state power supply operating at 16 kHz pulse repetition rate was employed [8].

2. Laser design and experimental arrangement

Figures 1 and 2 show the schematic and the photograph of the developed 110 W average power copper HyBrID laser. The laser was based on an air-cooled fused silica discharge tube of bore diameter ∼6 cm and length ∼200 cm. Its both ends were flared to reduce stress on the O-ring for vacuum sealing. High-purity cylindrical copper electrodes, press-fitted into water cooled stainless steel end flanges, were attached to its both ends using Viton O-rings. A very thin layer of alumina fibre insulation was wrapped suitably around the tube to maintain the desired temperature. Several high purity copper pieces were placed inside the discharge tube at regular intervals of ∼10 cm. Three aluminum strips, connected coaxially along the discharge tube, served as low-inductance current return.

A pair of single-side anti-reflection (AR) coated fused silica disks ($R \sim 4\%$), attached to the ends of the electrodes by Viton O-rings at ∼5° inclination with respect to the laser tube axis, served as the end windows. An HBr–neon gas mixing/monitoring system, consisting of a mass flow controller for neon and a fine metering valve for HBr, was used to inject a controlled quantity of gas mixture directly into the end of the discharge tube through a tygon-fused silica capillary feed-through.

In-situ reaction of the flowing HBr gas with hot copper pellets produced copper bromide molecules/vapour. This sublimed into the discharge followed by electron impact dissociation to produce copper atoms as the lasing species. The optical resonator consisted of a high reflecting plane mirror ($R > 99\%$) and an uncoated fused

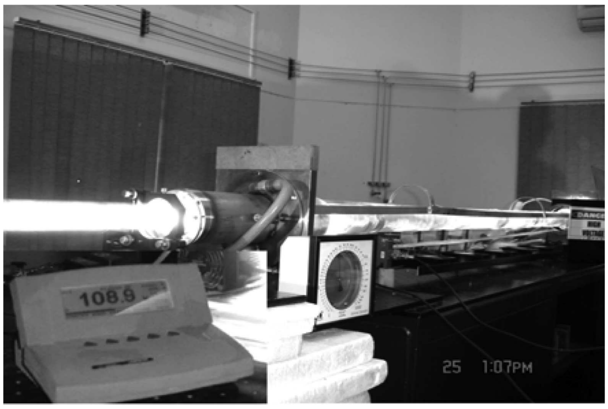

Figure 2. A 110 W copper HyBrID laser in operation.

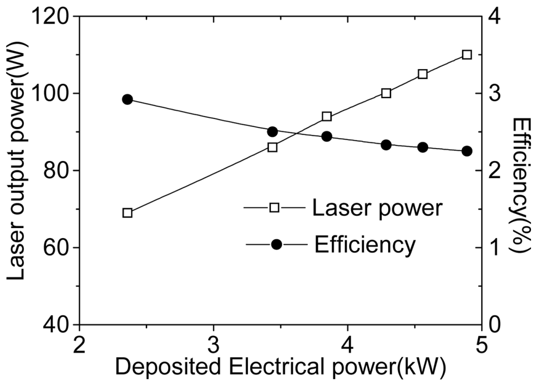

Figure 3. Variation of laser power and tube efficiency with deposited electrical power.

silica blank ($R \sim 7\%$). The laser discharge voltage and current were monitored using a 75 MHz high voltage probe (Tektronix-P6015A) and a fast current transformer (Pearson 110 A) respectively. All these pulses including the laser pulses taken by bi-planer phototubes (Hamamatsu-R1193U-52), were recorded using a 500 MHz digital oscilloscope (Tektronix-TDS 540 D). The laser output powers were measured using a thermal power meter (Ophir-LaserStar-FL250A-RP-SH).

3. Results and discussion

Figure 3 shows the variation of laser average output power and tube efficiency vs. electrical input power deposited at the laser head. The electrical power deposition was estimated in a procedure detailed in §4. Throughout the experiment, the total gas pressure (neon+HBr) (p) was set at an optimized value of ~35 mbar. The neon gas flow rate was set at ~6 l-atm/h. The HBr concentration was optimized at each

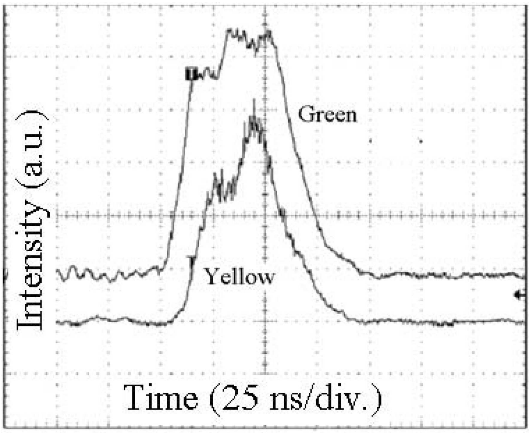

Figure 4. Temporal profile of green and yellow components of the copper HyBrID laser.

input power level and at the maximum output power level, it was ∼6% of the total gas pressure. As the deposited power increased from ∼2.4 to ∼4.9 kW, the laser output power increased monotonically from 70 to 110 W. But, the corresponding tube efficiency decreased from 2.9 to 2.2%. With increase in deposited power, the corresponding optimum HBr concentration also increased [2]. This has resulted in the production of larger amount of copper bromide vapour. Therefore, a larger fraction of copper atoms contributed to population inversion, hence the laser output power increased. On the other hand, the larger input power resulted in larger current density through the discharge tube. This decreased the fraction of the upper laser level pumping due to cumulative effect of increased rate of ionization of copper and metastable population. In addition to this, increased input power resulted in higher average gas temperature. This in turn altered the equilibrium concentration of HBr and its dissociation products (H_2, Br_2) [3]. Therefore, the beneficial effect of HBr, i.e., faster reduction of interpulse electron density by a process of dissociative attachment with low energy electrons (HBr + $e \rightarrow$ H + Br^- or H^- + Br) followed by the recovery of ground-state copper density by ion–ion neutralization (Cu^++ $Br^- \rightarrow$ Cu + Br and Cu^+ + $H^- \rightarrow$ Cu + H), was suppressed [1,9]. Hence the decrease in the laser efficiency, at higher input powers, was the combined effect of the above two processes. At 110 W laser power level, the near-field laser beam diameter was ∼4 cm which was about ∼30% less than the discharge tube bore diameter. At the maximum laser power, 110 W, the switched power ($0.5C_{\rm s}V_{C_{\rm s}}^2 f_{\rm s}$ where C_s is the storage capacitance, $V_{C_{\rm s}}$ is the voltage across $C_{\rm s}$ and $f_{\rm s}$ is the pulse repetition rate) was ∼10 kW. The input power beyond this was not increased in order to be within safe limit of the pulser, though figure 3 indicates a scope of improvement of the laser power with further increment of deposited electrical power.

At the total laser power of 110 W, the green and yellow component powers were 70 and 40 W respectively. Figure 4 shows the temporal evolution of laser intensity profile of both the radiation components, green and yellow, of this laser. The laser

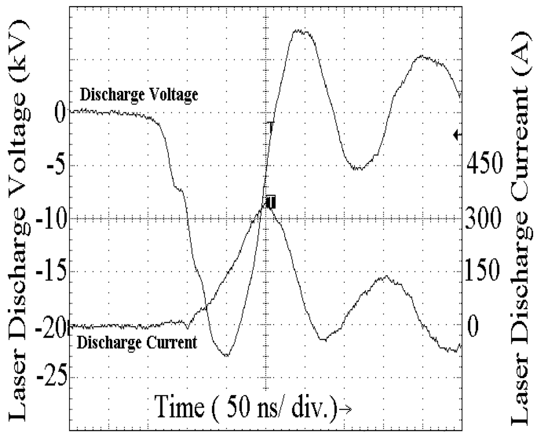

Figure 5. Temporal behaviour of the laser head voltage and current at 110 W laser power condition.

pulse widths (FWHM) of the green and yellow components were ∼50 ns and ∼40 ns respectively. These figures were ∼50% larger than the equivalent high temperature variant elemental CVL. Longer gain duration of copper HyBrID laser was attributed to relatively less depletion of ground state copper atoms to metastable level due to its lower operating temperature hence lower gas temperature [2,5].

Figure 5 shows the temporal behaviour of the recorded laser discharge voltage (V) and current waveforms (I) at 110 W laser power condition. The peak laser head voltage and current were ∼23 kV and ∼360 A respectively with a current pulse rise time of ∼80 ns. The reduced electric field (E/p), on which the electron energy distribution largely depends, was ∼3.33 V/cm-mbar. But, these values were less compared to the optimum E/p of 3.7–4.9 V/cm-mbar with a current pulse rise time of ∼60 ns required for this kind of devices [2]. This points to hope for further improvement in laser power.

4. Electrical power deposition at laser head

The solid-state pulser contained several elements such as a pulsed transformer, MPCs etc., which introduced losses when the electrical power was transferred from the storage capacitor to the laser head [8]. The typical MPCs used in CVL systems alone introduced 10–20% power loss per stage [1]. So a first-hand estimation of the electrical powers deposited at the laser head, at various switching power levels, were carried out from the numerical processing of laser head voltage and current waveforms [10,11]. For simplicity of the analysis, the voltage drop due to the electrical circuit loop inductance was not taken into account. The onset of the discharge voltage was used as reference point for timing. The waveforms (figure 5) were converted to point data with 10 ns resolution. The instantaneous power dumped, $P(t)$, at the laser head was estimated as

$$P(t) = V(t)I(t),$$

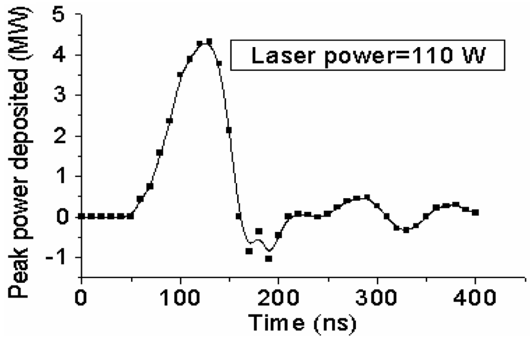

Figure 6. Temporal variation of the peak-deposited power in the laser tube at 110 W output power.

where $V(t)$ is the instantaneous laser head voltage and $I(t)$ is the instantaneous laser head current. The pulse energy dumped at the laser head, E_{p}, is given by

$$E_{\mathrm{p}} = \int P(t)\,\mathrm{d}t,$$

where t runs from 0 to $1/f_{\mathrm{s}}$. But, the majority of electrical power was dumped in initial 400 ns, hence we have taken t = 0–400 ns. The average power dumped at the laser head was estimated as

$$P_{\mathrm{dump}} = E_{\mathrm{p}} f_{\mathrm{s}}.$$

Figure 6 shows the typical variation of electrical power deposition at 110 W laser power condition. For the initial ∼50 ns, there was no power deposition because of the almost zero value of current. For the next ∼100 ns however, there is a resonant power deposition at the laser head. Further, it was the oscillatory behaviour of reduced amplitude. The corresponding deposited pulse energy and input power were estimated to be ∼306 mJ and ∼4.9 kW respectively. Similar estimations were carried out at all switching powers.

5. Conclusion

In conclusion, a copper HyBrID laser delivering 110 W average output power with 2.2% tube efficiency operating at 16 kHz pulse repetition rate was developed. The laser tube efficiency of 2.2%, achieved at this power level, was significantly higher than that of high temperature variant CVL. Maximum tube efficiency of 2.9% was observed at 70 W laser power level. At 110 W laser power condition, the laser pulse width was ∼50 ns (FWHM).

Acknowledgement

The authors acknowledge C Mukherjee for the AR coating of the laser windows and Shailendra Singh for power supply maintenance.

References

[1] C E Little (ed), *Metal vapour lasers* (John Wiley and Sons, Chichester, England, 1999)
[2] D R Jones, N V Sabotinov, A Maitland and C E Little, *Opt. Commun.* **94**, 289 (1992)
[3] E L Guyadec, P Coutance, G Bertrand and C Peltier, *IEEE J. Quantum Electron.* **35**(11), 1616 (1999)
[4] Akira Ohzu, Massaki Kato and Yoichiro Maruyama, *Appl. Phys. Lett.* **76(21)**, 2979 (2000)
[5] David R Jones, A Maitland and C E Little, *IEEE J. Quantum Electron.* **30(10)**, 2385 (1994)
[6] R Biswal, P K Agrawal, S V Nakhe, S K Dixit and J K Mittal, in *Lasers and Bose Einstein condensation physics* edited by Man Mohan, Anil Kumar, A B Bhattacharjee and A K Razdan (Narosa Publishing house, New Delhi, 2010) pp. 149–160
[7] R Biswal, P K Agrawal, S K Dixit and J K Mittal, *Proc. DAE-BRNS NLS-5*, 39 (2005)
[8] P K Agrawal, S V Nakhe, R Biswal and J K Mittal, in: *Book of abstracts*, Ninth DAE-BRNS National Laser Symposium (NLS-09), CP-01-06, 45 (2010)
[9] K I Zemskov, A A Isaev and G G Petrash, *Quantum Electron.* **27(7)**, 579 (1997)
[10] A I Isaev, D R Jones, C E Little, G G Petrash, C Whyte and K Zemskov, *IEEE J. Quantum Electron.* **33(6)**, 919 (1997)
[11] S V Nakhe, B S Rajanikanth and R Bhatnagar, *Meas. Sci. Technol.* **14**, 607 (2003)